Available online at www.sciencedirect.com

SciVerse ScienceDirect

Ceramics International 39 (2013) 6937–6943

CERAMICS INTERNATIONAL

www.elsevier.com/locate/ceramint

Synthesis and electrochemical characteristics of $LiNi_{0.5}Co_{0.5}O_2$ from different combinations of carbonates and oxides

Myoung Youp Song[a,*], Ho Rim[b], Hye Ryoung Park[c]

[a]Division of Advanced Materials Engineering, Hydrogen & Fuel Cell Research Center, Engineering Research Institute, Chonbuk National University, 567 Baekje-daero Deokjin-gu Jeonju, 561-756, Republic of Korea

[b]ASE Korea, 494 Munbal-dong Paju-si Gyeonggi-do, 413-790, Republic of Korea

[c]School of Applied Chemical Engineering, Chonnam National University, 300 Yongbong-dong Buk-gu Gwangju, 500-757, Republic of Korea

Received 7 January 2013; received in revised form 26 January 2013; accepted 12 February 2013
Available online 19 February 2013

Abstract

Cathode materials with a composition of $LiNi_{0.5}Co_{0.5}O_2$ were synthesized by a solid-state reaction method at 850 °C using Li_2CO_3, NiO or $NiCO_3$, and $CoCO_3$ or Co_3O_4, as the sources of Li, Ni, and Co, respectively. Electrochemical properties, structure, and microstructure of the synthesized $LiNi_{0.5}Co_{0.5}O_2$ samples were analyzed. The curves of voltage vs. x in $Li_xNi_{0.5}Co_{0.5}O_2$ for the first charge–discharge and the intercalated and deintercalated Li quantity Δx were studied. The destruction of unstable 3b sites and phase transitions are discussed from the first and second charge–discharge curves of voltage vs. x in $Li_xNi_{0.5}Co_{0.5}O_2$. The $LiNi_{0.5}Co_{0.5}O_2$ sample synthesized from Li_2CO_3, NiO, and Co_3O_4 has the largest first discharge capacity (159 mAh/g), with a discharge capacity deterioration rate of 5.8 mAh/g/cycle.

Keywords: $LiNi_{0.5}Co_{0.5}O_2$; Solid-state reaction method; Various starting materials; Curve of voltage vs. x in $Li_xNi_{0.5}Co_{0.5}O_2$; Discharge capacity

1. Introduction

Many researchers have been interested in $LiCoO_2$ [1–5], $LiNiO_2$ [6–13], and $LiMn_2O_4$ [14–20] as cathode materials for lithium secondary batteries [21]. $LiMn_2O_4$ contains a relatively inexpensive element, Mn, and is environment-friendly, but its cycling performance is poor. $LiCoO_2$ has a large diffusivity and a high operating voltage, and it can be synthesized relatively easily. However, it has a disadvantage in that it contains an expensive element, Co.

$LiNiO_2$ has a large discharge capacity [22], and is relatively excellent economically and environmentally. However, since Li and Ni have similar sizes ($Li^+ = 0.72$ Å and $Ni^{2+} = 0.69$ Å), $LiNiO_2$ is usually obtained in non-stoichiometric compositions, $Li_{1-y}Ni_{1+y}O_2$ [23,24]. The Ni^{2+} ions in the lithium planes obstruct the movement of the Li^+ ions during intercalation and deintercalation [5,26].

The shortcomings of $LiCoO_2$ and $LiNiO_2$ were overcome by incorporating $LiCoO_2$ and $LiNiO_2$ phases into $LiNi_{1-y}Co_yO_2$ compositions because the presence of cobalt stabilizes the structure in a strictly two-dimensional fashion, thus favoring good reversibility of the intercalation and deintercalation reactions [25,27–39]. Rougier et al. [25] reported that the stabilization of the two-dimensional character of the structure by cobalt substitution in $LiNiO_2$ is correlated with an increase in the cell performance, due to the decrease in the amount of extra nickel ions in the inter-slab space which impede the lithium diffusion. Kang et al. [39] investigated the structure and electrochemical properties of the $Li_xCo_yNi_{1-y}O_2$ ($y = 0.1$, 0.3, 0.5, 0.7 and 1.0) system synthesized by solid-state reaction with various starting materials to optimize the characteristics and synthetic conditions of the $Li_xCo_yNi_{1-y}O_2$. The first discharge capacities of $Li_xCo_yNi_{1-y}O_2$ were 60–180 mAh/g depending on synthesis conditions.

Solid-state reaction method [40,41], coprecipitation method [42], sol–gel method [43], ultrasonic spray pyrolysis method [44], combustion method [11], and emulsion method [45] have

*Corresponding author. Tel.: +82 63 270 2379; fax: +82 63 270 2386.
E-mail addresses: songmy@jbnu.ac.kr, songmy@chonbuk.ac.kr (M.Y. Song).

0272-8842/$ - see front matter © 2013 Elsevier Ltd and Techna Group S.r.l. All rights reserved.
http://dx.doi.org/10.1016/j.ceramint.2013.02.030

been reported for the synthesis of $LiNiO_2$ and $LiNi_{1-y}Co_yO_2$. The solid-state reaction method, which is quite simple, was used in this work.

To synthesize $LiNi_{1-y}Co_yO_2$ by the solid-state reaction method [25,27–30,32–34,37–39,46], different starting materials have been used by researchers. $LiOH \cdot H_2O$ or Li_2CO_3, NiO or $NiCO_3$, and Co_3O_4 or $CoCO_3$ have been used as starting materials by some researchers [37–39,46].

In this work, $LiNi_{0.5}Co_{0.5}O_2$ cathode materials were synthesized by a solid-state reaction method at 850 °C using Li_2CO_3, NiO or $NiCO_3$, and $CoCO_3$ or Co_3O_4 as the sources of Li, Ni, and Co, respectively. The electrochemical properties of the synthesized samples were then investigated. The structure of the synthesized $LiNi_{0.5}Co_{0.5}O_2$ was analyzed, and the microstructures of the samples were observed. The curves of voltage vs. x in $Li_xNi_{0.5}Co_{0.5}O_2$ for the first charge–discharge and the intercalated and deintercalated Li quantity Δx were studied. The destruction of unstable 3b sites and phase transitions were discussed from the first and second charge–discharge curves of voltage vs. x in $Li_xNi_{0.5}Co_{0.5}O_2$.

2. Experimental

Li_2CO_3, NiO or $NiCO_3$, and $CoCO_3$ or Co_3O_4 were used as starting materials in order to synthesize $LiNi_{0.5}Co_{0.5}O_2$ by the solid-state reaction method. All the starting materials (with purities of 99.9%) were purchased from Aldrich Co.

Fig. 1 schematically shows the experimental procedure for the synthesis of $LiNi_{0.5}Co_{0.5}O_2$ from Li_2CO_3, NiO or $NiCO_3$, and $CoCO_3$ or Co_3O_4 as the sources of Li, Ni, and Co, respectively, and the characterization of the synthesized samples. The mixture of the starting materials with the composition of $LiNi_{0.5}Co_{0.5}O_2$ was sufficiently mixed and pelletized. The pellet was then heat-treated in air at 650 °C for 20 h. It was then ground, mixed, pelletized, and calcined at 850 °C for 20 h. Then, this pellet was cooled at a rate of 50 °C/min, and then ground, mixed, and pelletized again. Finally, it was calcined again at 850 °C for 20 h.

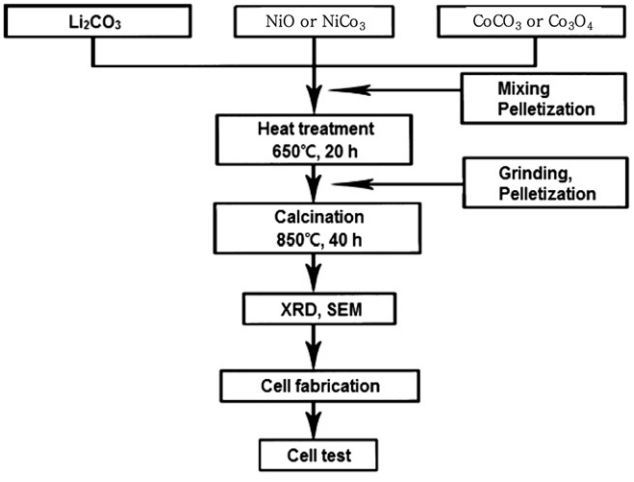

Fig. 1. Experimental procedure for $LiNi_{0.5}Co_{0.5}O_2$ synthesis from Li_2CO_3, NiO or $NiCO_3$, and $CoCO_3$ or Co_3O_4 as the sources of Li, Ni, and Co, respectively, and the characterization of the synthesized $LiNi_{0.5}Co_{0.5}O_2$.

The phase identification of the synthesized samples was carried out by X-ray Diffraction (XRD) analysis using CuK_α radiation (Mac-Science Co., Ltd.). The scanning rate was 16°/min, and the scanning range of the diffraction angle (2θ) was $10° \le 2\theta \le 70°$. The morphologies of the samples were observed using a scanning electron microscope (SEM).

Electrochemical cells consisted of $LiNi_{0.5}Co_{0.5}O_2$ as a positive electrode, Li foil as a negative electrode, and an electrolyte of 1 M $LiPF_6$ in a 1:1 (volume ratio) mixture of Ethylene Carbonate (EC) and Dimethyl Carbonate (DMC). Whatman glass-fiber was used as the separator. The cells were assembled in an argon-filled dry box. To fabricate the positive electrode, 89 wt% synthesized oxide, 10 wt% acetylene black, and 1 wt% Polytetrafluoroethylene (PTFE) binder were mixed in an agate mortar. By introducing Li metal, Whatman glass-fiber, the positive electrode, and the electrolyte, the cell was assembled. All the electrochemical tests were performed at room temperature with a potentiostatic/galvanostatic system (Mac-Pile system, Bio-Logic Co. Ltd.). The cells were cycled at a current density of 200 μA/cm^2 in a voltage range of 3.2–4.3 V.

3. Results and discussion

The XRD patterns of the $LiNi_{0.5}Co_{0.5}O_2$ and $LiCoO_2$ powders calcined at 850 °C for 40 h using Li_2CO_3, $NiCO_3$ and $CoCO_3$ as starting materials are shown in Fig. 2. The peaks are identified as corresponding to those of the $LiNiO_2$ phase, which has α-$NaFeO_2$ structure with a space group of $R\bar{3}m$. The fraction of each phase from the intensity ratios of the 003 and 104 peaks can be calculated since the 003 peak originates from the diffraction of only the $R\bar{3}m$ α-$NaFeO_2$ structure while the 104 peak originates from the diffractions of both the $R\bar{3}m$ α-$NaFeO_2$ and $Fm\bar{3}m$ NaCl structures. The value of the intensity ratio of

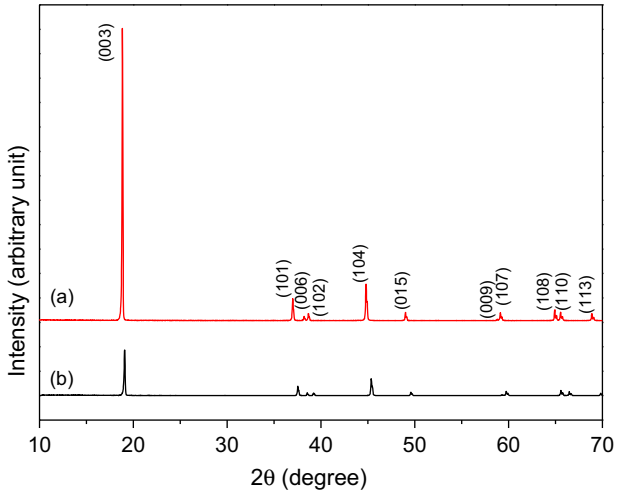

Fig. 2. X-ray (CuKα) diffraction patterns of (a) $LiNi_{0.5}Co_{0.5}O_2$ and (b) $LiCoO_2$ synthesized from Li_2CO_3, $NiCO_3$, and $CoCO_3$.

the 003 and 104 peaks, I_{003}/I_{104}, of the completely stoichiometric composition $LiNiO_2$ was reported to be about 1.3 by Morales et al. [24]. Ohzuku et al. [40] reported that the intensity ratio of the 003 and 104 peaks is a key parameter of the degree of displacement of the nickel and lithium ions. As the intensity ratio of the 003 and 104 peaks increases, the degree of displacement of the nickel and lithium ions decreases. They also reported that electroactive $LiNiO_2$ showed a clear split of the (108) and (110) lines, which appear in their XRD patterns at a diffraction angle near $2\theta = 65^\circ$. The XRD pattern of the $LiNi_{0.5}Co_{0.5}O_2$ powder synthesized using $LiCO_3$, $NiCO_3$, and $CoCO_3$, exhibited in Fig. 2, shows that the intensity ratio of the 003 and 104 peaks is quite high and exhibits a clear split of the (108) and (110) lines.

Fig. 3 shows the SEM micrographs of the $LiNi_{0.5}Co_{0.5}O_2$ synthesized at 850 °C from combinations of starting materials: (a) Li_2CO_3, NiO, and $CoCO_3$, (b) Li_2CO_3, NiO, and Co_3O_4, (c) Li_2CO_3, $NiCO_3$, and Co_3O_4, and (d) Li_2CO_3, $NiCO_3$, and $CoCO_3$. Overall, the sample (b) has the largest particles, followed in order by sample (a), sample (d), and sample (c). The surfaces of the particles of sample (b) are flat, while those of sample (a) are round. The particles of the samples (c) and (d) are agglomerated.

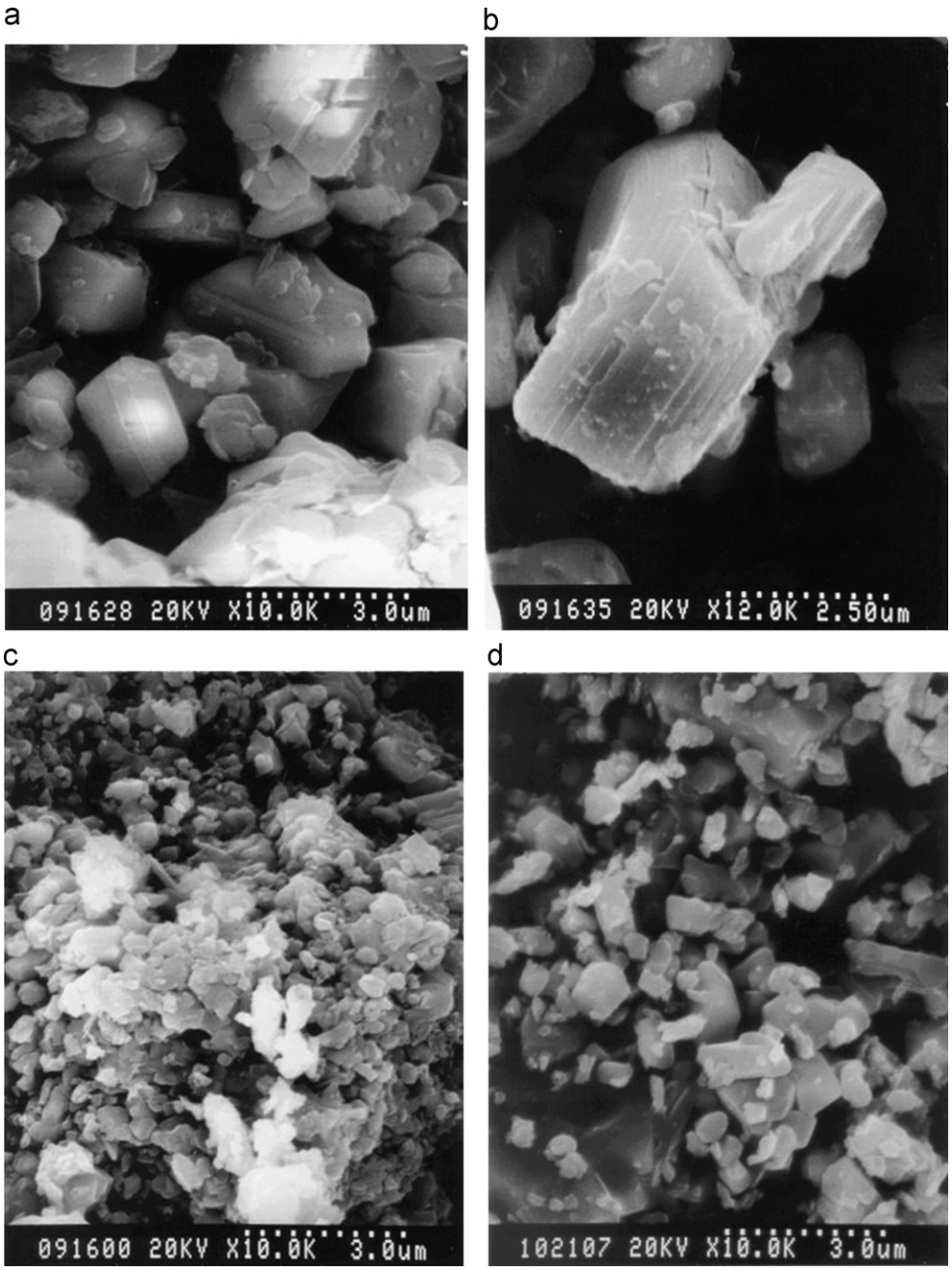

Fig. 3. SEM micrographs of the $LiNi_{0.5}Co_{0.5}O_2$ synthesized at 850 °C from combinations of starting materials: (a) Li_2CO_3, NiO, and $CoCO_3$, (b) Li_2CO_3, NiO, and Co_3O_4, (c) Li_2CO_3, $NiCO_3$ and Co_3O_4, and (d) Li_2CO_3, $NiCO_3$, and $CoCO_3$.

The curves of voltage vs. x in $Li_xNi_{0.5}Co_{0.5}O_2$ at a current density of 200 μA/cm^2 for the first charge–discharge of $LiNi_{0.5}Co_{0.5}O_2$ synthesized at 850 °C from combinations of starting materials are shown in Fig. 4, for: (a) Li_2CO_3, NiO, and $CoCO_3$, (b) Li_2CO_3, NiO, and Co_3O_4, (c) Li_2CO_3, $NiCO_3$, and Co_3O_4, and (d) Li_2CO_3, $NiCO_3$, and $CoCO_3$.

Polarization is a change in the potentials for the deintercalation and intercalation of lithium atoms. The samples (a), (b), and (d) have smaller polarization than sample (c). The charge or discharge capacity is proportional to the value of Δx in $Li_xNi_{0.5}Co_{0.5}O_2$. The sample (b) has the largest discharge capacity, followed in order by sample (d), sample (a), and sample (c).

Fig. 5 shows the curves of voltage vs. x in $Li_xNi_{0.5}Co_{0.5}O_2$ for the first and second charge–discharge cycles for $LiNi_{0.5}Co_{0.5}O_2$ synthesized at 850 °C from Li_2CO_3, NiO, and Co_3O_4. The value of Δx for the second discharge is slightly smaller than that for the first discharge.

The variations of the discharge capacity with number of cycles (n) for $LiNi_{0.5}Co_{0.5}O_2$ synthesized at 850 °C from (a) Li_2CO_3, NiO, and $CoCO_3$, (b) Li_2CO_3, NiO, and Co_3O_4, (c) Li_2CO_3, $NiCO_3$, and Co_3O_4, and (d) Li_2CO_3, $NiCO_3$, and $CoCO_3$ are shown in Fig. 6. The sample (b) has the largest first discharge capacity, followed in order by sample (d), sample (a), and sample (c). The sample (b) had the largest particles, which have the shape of polyhedron with flat surfaces. The sample (c) has the best cycling performance, followed in order by the samples (a), (b), and (d).

Fig. 7 shows the variations of the first-discharge capacity and the capacity deterioration rate of the $LiNi_{0.5}Co_{0.5}O_2$ synthesized at 850 °C with the following combinations of starting materials: (a) Li_2CO_3, NiO, and $CoCO_3$, (b) Li_2CO_3, NiO, and Co_3O_4, (c) Li_2CO_3, $NiCO_3$, and Co_3O_4, and (d) Li_2CO_3, $NiCO_3$, and $CoCO_3$. The sample (b) has the largest first-discharge capacity (159 mAh/g), followed in order by sample (d) (132 mAh/g), sample (a) (95 mAh/g), and sample (c) (72 mAh/g). The sample (c) has the smallest capacity deterioration rate (0.3 mAh/g/cycle), followed in order by sample (a) (3.0 mAh/g/cycle), sample (b) (5.8 mAh/g/cycle), and sample (d) (7.9 mAh/g/cycle). Over all, a sample with a larger first-discharge capacity has a larger capacity deterioration rate.

The curves of the voltage vs. x in $Li_xNi_{0.5}Co_{0.5}O_2$ at a current density of 200 μA/cm^2 for the first charge–discharge of $LiNi_{0.5}Co_{0.5}O_2$ in Fig. 4 show that, compared with the

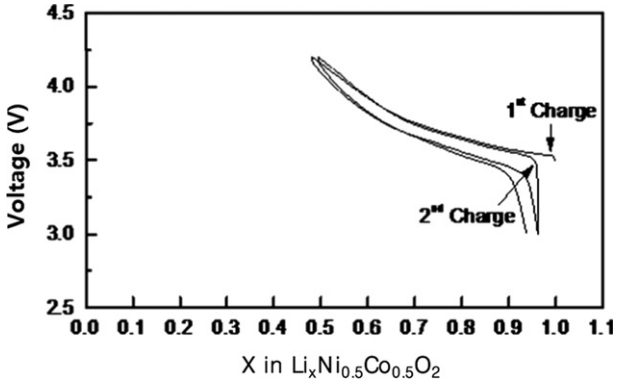

Fig. 5. Curves of voltage vs. x in $Li_xNi_{0.5}Co_{0.5}O_2$ for the first and second charge–discharge cycles for $LiNi_{0.5}Co_{0.5}O_2$ synthesized at 850 °C from Li_2CO_3, NiO, and Co_3O_4.

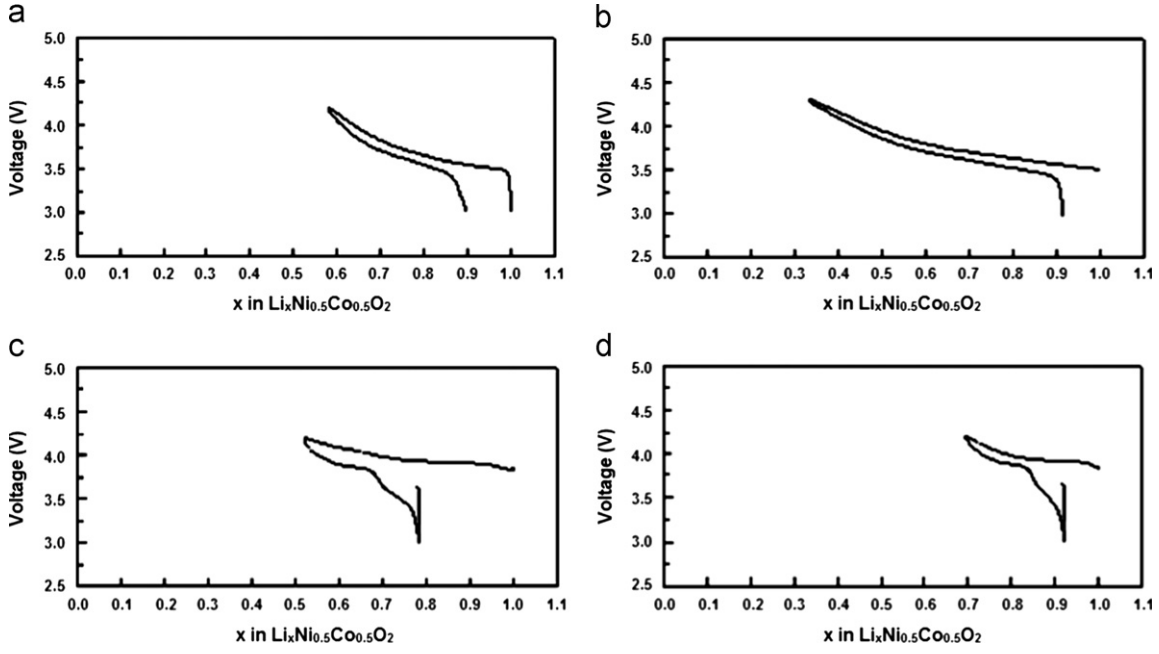

Fig. 4. Curves of voltage vs. x in $Li_xNi_{0.5}Co_{0.5}O_2$ at a current density of 200 μA/cm^2 for the first charge–discharge of $LiNi_{0.5}Co_{0.5}O_2$ synthesized at 850 °C from combinations of starting materials: (a) Li_2CO_3, NiO, and $CoCO_3$, (b) Li_2CO_3, NiO, and Co_3O_4, (c) Li_2CO_3, $NiCO_3$, and Co_3O_4 and (d) Li_2CO_3, $NiCO_3$, and $CoCO_3$.

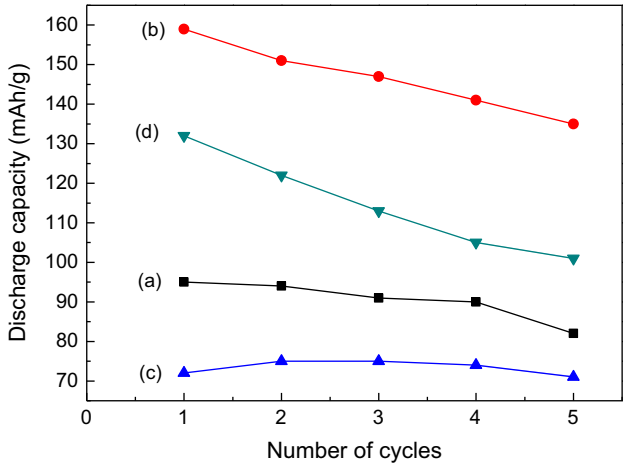

Fig. 6. Variations of the discharge capacity with number of cycles (n) for $LiNi_{0.5}Co_{0.5}O_2$ synthesized at 850 °C from (a) Li_2CO_3, NiO, and $CoCO_3$, (b) Li_2CO_3, NiO, and Co_3O_4, (c) Li_2CO_3, $NiCO_3$, and Co_3O_4 and (d) Li_2CO_3, $NiCO_3$, and $CoCO_3$.

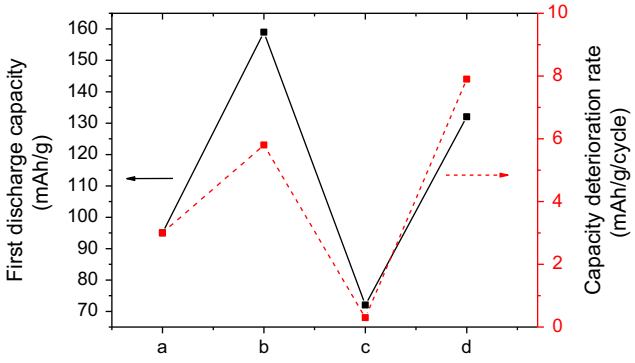

Fig. 7. Variations of the first discharge capacity and the capacity deterioration rate of the $LiNi_{0.5}Co_{0.5}O_2$ synthesized at 850 °C with combinations of starting materials: (a) Li_2CO_3, NiO, and $CoCO_3$, (b) Li_2CO_3, NiO, and Co_3O_4, (c) Li_2CO_3, $NiCO_3$, and Co_3O_4 and (d) Li_2CO_3, $NiCO_3$, and $CoCO_3$.

quantity of the deintercalated Li ions by the first charging, that of the intercalated Li ions by the first discharging is much smaller, which is revealed by the difference in Δx of the first charge and discharge curves for this sample. The lengths of plateaus in the charge and discharge curves are proportional to the charge and discharge capacities. During the first charging, Li ions deintercalate not only from stable 3b sites but also from unstable 3b sites. After deintercalation from unstable 3b sites, the unstable 3b sites will be destroyed. This is considered to lead to smaller quantity of the Li ions intercalated by the first discharging than that of the Li ions deintercalated by the first charging.

The curves of the voltage vs. x in $Li_xNi_{0.5}Co_{0.5}O_2$ for the first and second charge–discharge of $LiNi_{0.5}Co_{0.5}O_2$ synthesized at 850 °C from Li_2CO_3, NiO and Co_3O_4 in Fig. 5 show that the difference in Δx of the second charge and discharge curves is smaller than that of the first charge and discharge curves. This shows that the destruction of unstable 3b sites occurs less severely at the second cycle than at the first cycle.

In the curves of the voltage vs. x in $Li_xNi_{0.5}Co_{0.5}O_2$ for the first and second charge–discharge of $LiNi_{0.5}Co_{0.5}O_2$ synthesized at 850 °C from Li_2CO_3, NiO, and Co_3O_4 in Fig. 5, the charge–discharge curves exhibit quite long plateaus, where two phases co-exist [47]. Arai et al. [48] reported that, during charging and discharging, $LiNiO_2$ goes through three phase transitions: from hexagonal structure (H1) to monoclinic structure (M), from monoclinic structure (M) to hexagonal structure (H2), and from hexagonal structure (H2) to hexagonal structure (H3), or vice versa. Ohzuku et al. [40] reported that during charging and discharging, $LiNiO_2$ goes through four phase transitions: from H1 to M, from M to H2, from H2 to hexagonal structures H2+H3, and from H2+H3 to H3, or vice versa. Song et al. [49] reported that—$dx/|dV|$ vs. V curves of $LiNi_{1-y}Ti_yO_2$ ($y=0.012$ and 0.025) for charging and discharging showed four peaks, revealing four phase transitions from H1 to M, from M to H2, from H2 to H2+H3, and from H2+H3 to H3, or vice versa.

The variations of the first discharge capacity and the capacity deterioration rate of the $LiNi_{0.5}Co_{0.5}O_2$ with combinations of starting materials given in Fig. 7 show that over all, a sample with a larger first discharge capacity has a larger capacity deterioration rate. A larger first discharge capacity corresponds to a larger amount of intercalation of Li, which is related to the wider change of the value of x in $Li_xNi_{0.5}Co_{0.5}O_2$. The larger change of the value of x will cause larger expansion and contraction of the $LiNiO_2$ phase with the α-$NaFeO_2$ structure due to the intercalation and deintercalation. This will make the unit cell strained and distorted. With cycling, the interstitial sites and thus the α-$NaFeO_2$ structure will be destroyed. This decreases the fraction of the $LiNiO_2$ phase, leading to the capacity fading of $LiNi_{0.5}Co_{0.5}O_2$ with cycling. For the samples with smaller discharge capacity, the expansion and contraction due to intercalation and deintercalation can be within the limit of elasticity of $LiNi_{0.5}Co_{0.5}O_2$, and the lattice destruction can thus be small. The discharge capacity can accordingly decrease slowly with cycling (i.e., the capacity fading rate can be low).

4. Conclusions

$LiNi_{0.5}Co_{0.5}O_2$ cathode materials were synthesized by a solid-state reaction method at 850 °C using Li_2CO_3, NiO or $NiCO_3$, and $CoCO_3$ or Co_3O_4 as the sources of Li, Ni, and Co, respectively. The electrochemical properties of the synthesized samples were then investigated. The $LiNi_{0.5}Co_{0.5}O_2$ sample synthesized from Li_2CO_3, NiO, and Co_3O_4 has the largest first discharge capacity (159 mAh/g) with a discharge capacity deterioration rate of 5.8 mAh/g/cycle. The curves of the voltage vs. x in $Li_xNi_{0.5}Co_{0.5}O_2$ for the first charge–discharge of $LiNi_{0.5}Co_{0.5}O_2$ showed that after deintercalation from unstable 3b sites, the unstable 3b sites will be destroyed, leading to a smaller quantity of the Li ions

intercalated by the first discharging than that of the Li ions deintercalated by the first charging. Over all, a sample with a larger first discharge capacity had a larger capacity deterioration rate. For samples with a smaller discharge capacity, the lattice destruction due to the expansion and contraction according to intercalation and deintercalation will be small. The capacity fading rate will be low accordingly.

References

[1] K. Ozawa, Lithium-ion rechargeable batteries with $LiCoO_2$ and carbon electrodes: the $LiCoO_2$/C system, Solid State Ionics 69 (1994) 212–221.

[2] R. Alcántara, P. Lavela, J.L. Tirado, R. Stoyanova, E. Zhecheva, Structure and electrochemical properties of boron-doped $LiCoO_2$, Journal of Solid State Chemistry 134 (1997) 265–273.

[3] Z.S. Peng, C.R. Wan, C.Y. Jiang, Synthesis by sol–gel process and characterization of $LiCoO_2$ cathode materials, Journal of Power Sources 72 (1998) 215–220.

[4] W.D. Yang, C.Y. Hsieh, H.J. Chuang, Y.S. Chen, Preparation and characterization of nanometric-sized $LiCoO_2$ cathode materials for lithium batteries by a novel sol–gel method, Ceramics International 36 (1) (2010) 135–140.

[5] S.K. Kim, D.H. Yang, J.S. Sohn, Y.C. Jung, Resynthesis of $LiCo_{1-x}Mn_xO_2$ as a cathode material for lithium secondary batteries, Metals and Materials International 18 (2) (2012) 321–326.

[6] J.R. Dahn, U. von Sacken, C.A. Michal, Structure and electrochemistry of $Li_{1\pm y}NiO_2$ and a new Li_2NiO_2 phase with the $Ni(OH)_2$ structure, Solid State Ionics 44 (1990) 87–97.

[7] J.R. Dahn, U. von Sacken, M.W. Juzkow, H. Al-Janaby, Rechargeable $LiNiO_2$/carbon cells, Journal of Electrochemical Society 138 (1991) 2207–2212.

[8] H.U. Kim, D.R. Mumm, H.R. Park, M.Y. Song, Synthesis by a simple combustion method and electrochemical properties of $LiCo_{1/3}Ni_{1/3}Mn_{1/3}O_2$, Electronic Materials Letters 6 (3) (2010) 91–95.

[9] S.H. Ju, J.H. Kim, Y.C. Kang, Electrochemical properties of $LiNi_{0.8}Co_{0.2-x}Al_xO_2$ $(0 \le x \le 0.1)$ cathode particles prepared by spray pyrolysis from the spray solutions with and without organic additives, Metals and Materials International 16 (2) (2010) 299–303.

[10] D.H. Kim, Y.U. Jeong, D.H. Kim, Y.U. Jeong, Crystal structures and electrochemical properties of $LiNi_{1-x}Mg_xO_2$ $(0 \le x \le 0.1)$ for cathode materials of secondary lithium batteries, Korean Journal of Metals and Materials 48 (3) (2010) 262–267.

[11] S.N. Kwon, J.H. Song, D.R. Mumm, Effects of cathode fabrication conditions and cycling on the electrochemical performance of $LiNiO_2$ synthesized by combustion and calcination, Ceramics International 37 (5) (2011) 1543–1548.

[12] M.Y. Song, C.K. Park, H.R. Park, D.R. Mumm, Variations in the electrochemical properties of metallic elements-substituted $LiNiO_2$ cathodes with preparation and cathode fabrication conditions, Electronic Materials Letters 8 (1) (2012) 37–42.

[13] M.Y. Song, D.R. Mumm, C.K. Park, H.R. Park, Cycling performances of $LiNi_{1-y}M_yO_2$ (M = Ni, Ga, Al and/or Ti) synthesized by wet milling and solid-state method, Metals and Materials International 18 (3) (2012) 465–472.

[14] J.M. Tarascon, E. Wang, F.K. Shokoohi, W.R. Mckinnon, S. Colson, The spinel phase of $LiMn_2O_4$ as a cathode in secondary lithium cells, Journal of the Electrochemical Society 138 (1991) 2859–2864.

[15] A.R. Armstrong, P.G. Bruce, Synthesis of layered $LiMnO_2$ as an electrode for rechargeable lithium batteries, Letters in Nature 381 (1996) 499–500.

[16] M.Y. Song, D.S. Ahn, On the capacity deterioration of spinel phase $LiMn_2O_4$ with cycling around 4 V, Solid State Ionics 112 (1998) 21–24.

[17] M.Y. Song, D.S. Ahn, H.R. Park, Capacity fading of spinel phase $LiMn_2O_4$ with cycling, Journal of Power Sources 83 (1999) 57–60.

[18] D.S. Ahn, M.Y. Song, Variations of the electrochemica properties of $LiMn_2O_4$ with synthesis conditions, Journal of the Electrochemical Society 147 (3) (2000) 874–879.

[19] H.J. Guo, Q.H. Li, X.H. Li, Z.X. Wang, W.J. Peng, Novel synthesis of $LiMn_2O_4$ with large tap density by oxidation of manganese powder, Energy Conversion and Management 52 (4) (2011) 2009–2014.

[20] C. Wan, M. Cheng, D. Wu, Synthesis of spherical spinel $LiMn_2O_4$ with commercial manganese carbonate, Powder Technology 210 (1) (2011) 47–51.

[21] J.W. Park, J.H. Yu, K.W. Kim, H.S. Ryu, J.H. Ahn, C.S. Jin, K.H. Shin, Y.C. Kim, H.J. Ahn, Surface morphology changes of lithium/sulfur battery using multi-walled carbon nanotube added sulfur electrode during cyclings, Korean Journal of Metals and Materials 49 (2) (2011) 174–179.

[22] Y. Nishida, K. Nakane, T. Satoh, Synthesis and properties of gallium-doped $LiNiO_2$ as the cathode material for lithium secondary batteries, Journal of Power Sources 68 (1997) 561–564.

[23] P. Barboux, J.M. Tarascon, F.K. Shokoohi, The use of acetates as precursors for the low-temperature synthesis of $LiMn_2O_4$ and $LiCoO_2$ intercalation compounds, Journa of Solid State Chem 94 (1991) 185–196.

[24] J. Morales, C. Perez-Vicente, J.L. Tirado, Cation distribution and chemical deintercalation of $Li_{1-x}Ni_{1+x}O_2$, Materials Research Bulletin 25 (1990) 623–630.

[25] A. Rougier, I. Saadoune, P. Gravereau, P. Willmann, C. Delmas, Effect of cobalt substitution on cationic distribution in $LiNi_{1-y}Co_yO_2$ electrode materials, Solid State Ionics 90 (1996) 83–90.

[26] B.J. Neudecker, R.A. Zuhr, B.S. Kwak, J.B. Bates, J.D. Robertson, Lithium manganese nickel oxides $Li_x(Mn_yNi_{1-y})_{2-x}O_2$, Journal of the Electrochemical Society 145 (1998) 4148–4157.

[27] C. Delmas, I. Saadoune, Electrochemical and physical properties of the $Li_xNi_{1-y}Co_yO_2$ phases, Solid State Ionics 53–56 (1992) 370–375.

[28] E. Zhecheva, R. Stoyanova, Stabilization of the layered crystal structure of $LiNiO_2$ by Co-substitution, Solid State Ionics 66 (1993) 143–149.

[29] C. Delmas, I. Saadoune, A. Rougier, The cycling properties of the $Li_xNi_{1-y}Co_yO_2$ electrode, Journal of Power Sources 43–44 (1993) 595–602.

[30] A. Ueda, T. Ohzuku, Solid-state redox reactions of $LiNi_{1/2}Co_{1/2}O_2$ ($R\bar{3}m$) for 4 V secondary lithium cells, Journal of the Electrochemical Society 141 (1994) 2010–2014.

[31] M. Menetrier, A. Rougier, C. Delmas, Cobalt segregation in the $LiNi_{1-y}Co_yO_2$ solid solution: a preliminary ^7Li NMR study, Solid State Commun. 90 (1994) 439–442.

[32] R. Alcantara, J. Morales, J.L. Tirado, R. Stoyanova, E. Zhecheva, Structure and electrochemical properties of $Li_{1-x}(Ni_yCo_{1-y})_{1+x}O_2$ Effect of chemical delithiation at 0 °C, Journal of the Electrochemical Society 142 (1995) 3997–4005.

[33] B. Banov, J. Bourilkov, M. Mladenov, Cobalt stabilized layered lithium–nickel oxides, cathodes in lithium rechargeable cells, Journal of Power Sources 54 (1995) 268–270.

[34] Y.M. Choi, S.I. Pyun, S.I. Moon, Effects of cation mixing on the electrochemical lithium intercalation reaction into porous $Li_{1-\delta}Ni_{1-y}Co_yO_2$ electrodes, Solid State Ionics 89 (1996) 43–52.

[35] S.J. Lee, J.K. Lee, D.W. Kim, H.K. Baik, S.M. Lee, Fabrication of thin film $LiCo_{0.5}Ni_{0.5}O_2$ cathode for Li rechargeable microbattery, Journal of the Electrochemical Society 143 (1996) L268–L270.

[36] D. Caurant, N. Baffier, B. Garcia, J.P. Pereira-Ramos, Synthesis by a soft chemistry route and characterization of $LiNi_xCo_{1-x}O_2$ $(0 \le x \le 1)$ cathode materials, Solid State Ionics 91 (1996) 45–54.

[37] H. Rim, H.R. Park, M.Y. Song, Synthesis of lithium $LiNi_{1-y}Co_yO_2$ from lithium carbonate, nickel oxide and cobalt carbonate and their electrochemical properties, Ceramics International 38 (2012) 5987–5991.

[38] H. Rim, H.R. Park, M.Y. Song, Electrochemical performance of cobalt-substituted lithium nickel oxides synthesized from lithium and nickel carbonates and cobalt oxide, Ceramics International 39 (2013) 917–923.

[39] S.G. Kang, K.S. Ryu, S.H. Chang, S.C. Park, The novel synthetic route to $LiCo_yNi_{1-y}O_2$ as a cathode material in lithium secondary batteries, Bulletin of the Korean Chemical Society 22 (12) (2001) 1328–1332.

[40] T. Ohzuku, A. Ueda, M. Nagayama, Electrochemistry and structural chemistry of $LiNiO_2$ ($R\bar{3}m$) for 4 V secondary lithium cells, Journal of the Electrochemical Society 140 (1993) 1862–1870.

[41] Z. Lu, X. Huang, H. Haung, L. Chen, J. Schoonman, The phase transition and optimal synthesis temperature of LiNiO2, Solid State Ionics 120 (1999) 103–107.

[42] M. Guilmard, A. Rougier, M. Grune, L. Croguennec, C. Delmas, Effects of aluminum on the structural and electrochemical properties of $LiNiO_2$, Journal of Power Sources 115 (2003) 305–314.

[43] B.J. Hwang, R. Santhanam, C.H. Chen, Effect of synthesis conditions on electrochemical properties of $LiCo_yNi_{1-y}O_2$ cathode for lithium rechargeable batteries, Journal of Power Sources 114 (2003) 244–252.

[44] S.H. Park, C.S. Yoon, S.G. Kang, H.S. Kim, S.I. Moon, Y.K. Sun, Synthesis and structural characterization of layered $Li[Ni_{1/3}Co_{1/3}Mn_{1/3}]O_2$ cathode materials by ultrasonic spray pyrolysis method, Electrochimica Acta 49 (2004) 557–563.

[45] B.H. Kim, J.H. Kim, I.H. Kwon, M.Y. Song, Electrochemical properties of $LiNiO_2$ cathode material synthesized by the emulsion method, Ceramics International 33 (2007) 837–841.

[46] M.Y. Song, H. Rim, E. Bang, Electrochemical properties of cathode materials $LiNi_{1-y}Co_yO_2$ synthesized using various starting materials, Journal of Applied Electrochem 34 (2004) 383–389.

[47] W. Li, J.N. Reimers, J.R. Dahn, In situ X-ray diffraction and electrochemical studies of $Li_{1-x}NiO_2$, Solid State Ionics 67 (1993) 123–130.

[48] H. Arai, S. Okada, H. Ohtsuka, M. Ichimura, J. Yamaki, Characterization and cathode performance of $Li_{1-x}Ni_{1+x}O_2$ prepared with the excess lithium method, Solid State Ionics 80 (1995) 261–269.

[49] M.Y. Song, D.S. Lee, H.R. Park, Electrochemical properties of $LiNi_{1-y}Ti_yO_2$ and $LiNi_{0.975}M_{0.025}O_2$ (M = Zn, Al, and Ti) synthesized by the solid-state reaction method, Materials Research Bulletin 47 (2012) 1021–1027.